5 Cournot Duopoly with Kinked Demand according to Palander and Wald

Tönu Puu [1], *Laura Gardini* [2], *and Irina Sushko* [3]

[1] Centre for Regional Science, University of Umeå, Sweden
[2] Department of Economics, University of Urbino, Italy
[3] Institute of Mathematics, National Academy of Sciences, Kiev, Ukraine

1 Introduction

In a short printed abstract of contributions to a Cowles Commission conference at Colorado Springs in 1936, and an extensive follow up, in Swedish, dating from 1939, Tord Palander focused some interesting dynamics problems in Cournot duopoly when the demand curve was kinked linear and the marginal revenue curve hence jumped up, producing two different local profit maximising intersections with the curve of marginal cost, which was assumed constant or even zero. The Cournot reaction functions, as well, then became piecewise linear, including a jump, and they could produce several, coexistent and locally stable equilibria. Palander specified the basins for these, though nor completely, and also the basin for initial conditions from which the system in stead went to an attractive 2-periodic oscillation.

For another case, where the reaction functions did not intersect, and there hence did not exist any Nash equilibrium, Palander recognised the existence of an attractive 3-periodic cycle. Given the numerical tools at that time, the accuracy of his calculations is in fact amazing, though he missed the coexistence of a 6-period cycle and again the complete characterisation of the basins.

Palander gave his argument in terms of two numerical cases, one with identical firms, another with a slight asymmetry between them.

It is noteworthy that, also in 1936, Abraham Wald considered the same type of problems, in an article which later became celebrated as first rigorous statement of existence problems for multi-market equilibria, left open by Walras and later elaborated by Arrow and Debreu.

Like Palander, Wald gave his argument in terms of two numerical examples, and also assumed the demand curve to start and end with straight line segments, but, unlike Palander, he did not assume the curves to meet under a sharp angle. Rather the two line segments were smoothly joined by either a circular segment, or by a demand curve where price was reciprocal to supply squared. The lines and curves were hence joined at tangency, so the demand function was not only continuous but differentiable. The first example, with a circular segment, seems miscalculated, but the second, hyperbola like, is most interesting, as it results in a nondenumerable infinity of coexistent Nash equilibria.

Given its context, Wald was not interested in the dynamics of the reaction functions. Had he cared to elaborate the dynamics, he would have found that none of the coexistent equilibria was even locally attractive. Rather the whole state space, except the sparse subset of the diagonal, would provide basins for oscillatory motions, quite as in Palander's cases, though all different and nondenumerably infinite in number.

It seems sufficiently interesting in itself to lift forward this neglected material, and completing the analysis. However, there is more to it. Sectional linearity of the demand function, combined with constant marginal costs, makes all falling segments of the reaction function have slope -1/2, and this makes all Nash equilibria stable. There may be cycles, even coexistent, but no such things as chaos. However, considering falling marginal costs, the slope becomes steeper, and we may in fact obtain much more interesting dynamics. Globally decreasing marginal costs, of course, do not make sense, but locally, as an approximation to the falling section of a U-shaped marginal cost curve, they indeed do.

We should note that, in all these cases, demand sensitivity to price goes up as price goes down. Joan Robinson in 1933 gave factual arguments for this, in terms of new and more numerous groups of consumers entering the market once they could afford the good, in fact the same type of assumptions as used in all textbook discussions of price discrimination.

The so called "kinked demand case" for duopoly is something quite different. There demand was assumed to become less, not more, elastic as price went down. The explanation for this was not in terms of behaviour of the consumers, but of the competitors, who were supposed to retaliate to increased demand, aimed at bringing price down, but not to reduced demand to bring about the reverse. This type of model was used to the purpose of explaining an allegedly observed extreme stability in duopoly pricing, and so had a strong flavour of ad hoc explanation. See Sweezy (1939). In this latter case the jump in marginal revenue was down, not up, but this is not the issue Palander and Wald dealt with, which no doubt is the more interesting.

2 Palander's First Case

In his first case Palander assumed two identical duopoly firms (both having zero average = marginal cost), facing the kinked (inverse) demand function:

$$p = f(q) = \begin{cases} 100 - \dfrac{q}{20} & q < 1800 \\ \dfrac{100}{7} - \dfrac{q}{420} & q > 1800 \end{cases} \tag{1}$$

shown as the broken black curve in Fig. 1. If we had dealt with a case of simple monopoly, the marginal revenue would have been:

$$MR = \begin{cases} 100 - \dfrac{q}{10} & q < 1800 \\ \dfrac{100}{7} - \dfrac{q}{210} & q > 1800 \end{cases} \tag{2}$$

as usual with the same intercepts as the bits of the demand function, but with doubled slope for each. This produces a jump up from -80 to 40/7 in the marginal revenue function at the kink point, i.e. for q = 1800, as we can calculate from (2).

With zero marginal cost we obtain two *local* profit maxima for the monopolist from $MR = MC = 0$, q = 1000 and q = 3000 respectively. The corresponding monopoly prices from (1) then become p = 50, and p = 100/21, and the profits (in absence of production costs) become pq = 50000 and pq = 150000/7, so it is obvious that the monopolist would select the first of the local maxima.

We can see the marginal revenue curve for the monopolist in Fig. 1 as the curve supported by the darkest shade area. Fig. 1 was drawn for a duopolist, but when one competitor supplies zero the other duopolist becomes a monopolist. The horizontal axis in the present case also is the marginal cost curve. It intersects the discontinuous marginal revenue curve in two points, the local profit maxima. Economists are used to establish the global maximum by comparing the triangular areas formed by the marginal revenue curve above and below the marginal cost curve (at present the zero line). It is obvi-

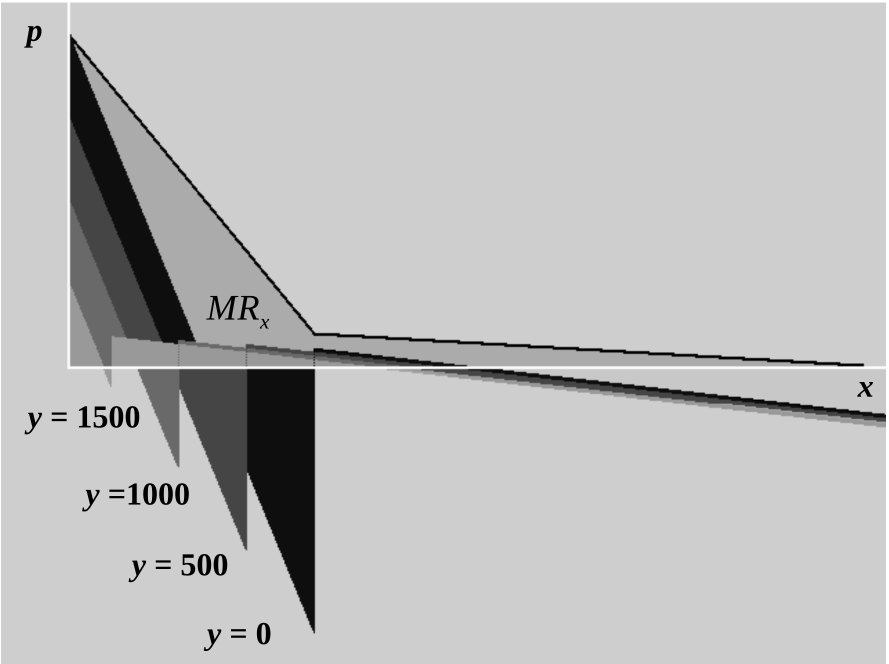

Fig. 1. Demand curve in Palander's first case, and marginal revenue curves for the first firm. Range for x: [0, 10000]*, range for p:* [0, 100].

ous that the loss area, below the axis, outweighs the gain area, above the axis, by several times, so that the lower intersection with the axis establishes the global optimum (as already demonstrated numerically). At least this is true with the darkest marginal revenue curve, for the case of monopoly, or zero supply by the competitor. We can already note that this is not always the case in duopoly with positive supplies by the competitor. As shown by the marginal revenue curves with support areas in brighter shade, it may be the higher intersection point that represents the global optimum provided the competitor supplies sufficiently much.

In duopoly, denote the supplies of the competitors, x and y, so $q = x + y$. Now the marginal revenue of the first firm is:

$$MR_x = \begin{cases} 100 - \dfrac{x}{10} - \dfrac{y}{20} & x < 1800 - y \\ \dfrac{100}{7} - \dfrac{x}{210} - \dfrac{y}{420} & x > 1800 - y \end{cases} \tag{3}$$

and likewise for the second firm:

$$MR_y = \begin{cases} 100 - \dfrac{x}{20} - \dfrac{y}{10} & y < 1800 - x \\ \dfrac{100}{7} - \dfrac{x}{420} - \dfrac{y}{210} & y > 1800 - x \end{cases} \tag{4}$$

As we see, the supply by the competitor subtracts from the intercept of the marginal revenue curve, and also pushes the kink point to the left. See Fig. 1. Note however that in equations (3)-(4) the competitor's supply enters with only half the coefficient of the duopolist's own supply. Hence, the presence of a positive supply by the competitor not only pushes the whole marginal revenue curve to the left, but it also decreases the size of the dip, thereby changing the loss and gain areas. As already noted it may be that the global optimum shifts from small supply to large when the competitor increases his supply.

To establish the local optimum, given zero marginal costs, the first firm solves the equation: $MR_x = MC_x = 0$ with respect to *x*, and the second firm solves the equation $MR_y = MC_y = 0$ with respect to *y*. This results in the reaction functions $x' = \phi(y)$ and $y' = \varphi(x)$, which we will expect to become identical in view of the symmetry of the present case. Equating (3) to zero gives us two solutions for $x' = \phi(y)$:

$$x' = \phi(y) = 1000 - \frac{y}{2} \tag{5}$$

$$x' = \phi(y) = 3000 - \frac{y}{2} \tag{6}$$

so we have to establish a criterion for the choice. (Note that the dash denotes advancing the map one step in a dynamical sense from *t* to *t* + 1.) There are now two different things to consider.

First, (5) and (6) are not applicable everywhere. We have to consider that (5) applies if $q < 1800$, (6) if $q > 1800$. Given $q = x + y$ we find by substitution from (5) in $q < 1800$ the condition $y < 1600$ for the validity of (5). Likewise, substituting from (6) in $q > 1800$, we find the condition $y > -2400$ for the validity of (6), which is not restrictive, as the supply *y* anyhow has to be nonnegative. So, we rephrase (5)-(6):

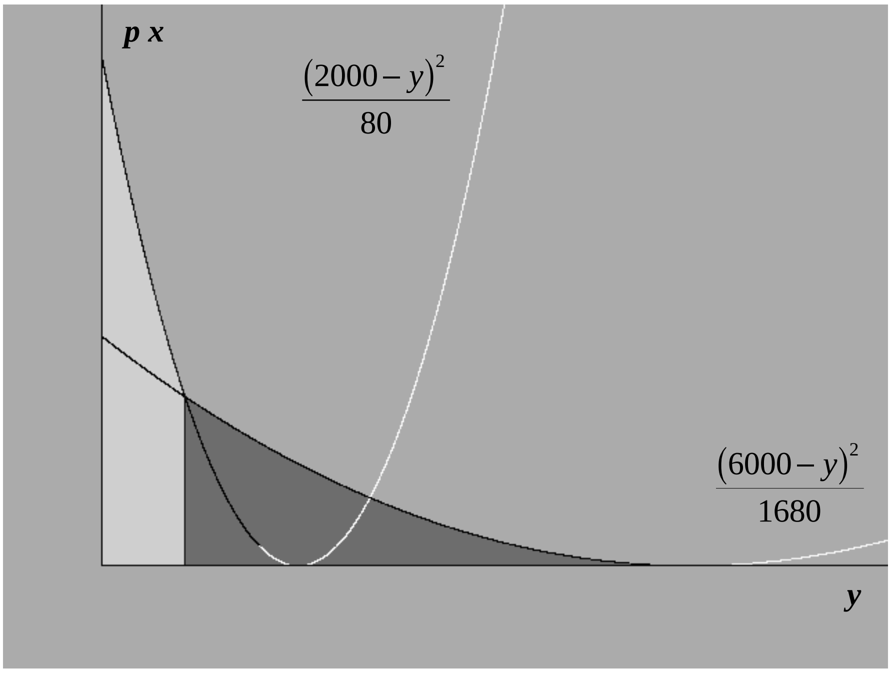

Fig. 2. Local profit maxima for the first firm as dependent on the competitor's supply. Black sections of the profit parabolas are the relevant ones. Range for y: [0, 7000], *range for px (profits):* [0, 55000].

$$x' = \phi(y) = 1000 - \frac{y}{2} \qquad y < 1600 \tag{7}$$

$$x' = \phi(y) = 3000 - \frac{y}{2} \qquad -2400 < y \tag{8}$$

Further, not only the supply of the competitor, but the supply of the firm itself has to be positive in order to make sense. From (5) we therefore find $y < 2000$, which is not operative because it is already implied by $y < 1600$. Likewise from (6) we find $y < 6000$, which, however, is. Consequently, considering all constraints, we can now write (7)-(8):

$$x' = \phi(y) = 1000 - \frac{y}{2} \qquad 0 < y < 1600 \tag{9}$$

$$x' = \phi(y) = 3000 - \frac{y}{2} \qquad 0 < y < 6000 \tag{10}$$

We are not quite done yet, because the expressions (9)-(10) have a common range of validity, $0 < y < 1600$, and so do not yield a unique solution in this interval. To achieve this we have to consider the following fact. Both solutions provide local profit maxima, but we have to select the global one.

As production costs are zero, profits equal revenues, so we obtain by substitution from (9) in (1):

$$px' = \frac{(2000 - y)^2}{80} \qquad 0 < y < 1600 \tag{11}$$

Similarly, substituting from (10) in (1):

$$px' = \frac{(6000 - y)^2}{1680} \qquad 0 < y < 6000 \tag{12}$$

Equating (11) to (12), we get two solutions:

$$y = 1800 \pm 200\sqrt{21} \tag{13}$$

but only the smaller root makes sense, as only this is in the common validity range $0 < y < 1600$. This always is the case when we compare profits. Even if we solve a second order equation only one root counts. The geometry of the case is illustrated in Fig. 2, where the dark curves are the relevant ones.

So, assembling the pieces we have:

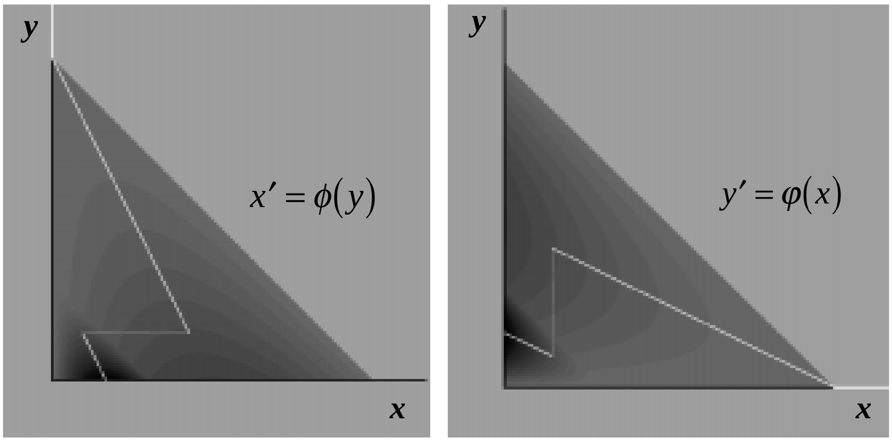

Fig. 3. Profit surfaces for the two firms in Palander's first case represented in terms of shading and the raction curves for the firms. Ranges for x, y: [0, 7000].

$$x' = \phi(y) = \begin{cases} 1000 - y/2 & 0 < y < 1800 - 200\sqrt{21} \\ 3000 - y/2 & 1800 - 200\sqrt{21} < y < 6000 \\ 0 & 6000 < y \end{cases} \qquad (14)$$

for the first firm, and likewise for the second firm:

$$y' = \varphi(x) = \begin{cases} 1000 - x/2 & 0 < x < 1800 - 200\sqrt{21} \\ 3000 - x/2 & 1800 - 200\sqrt{21} < x < 6000 \\ 0 & 6000 < x \end{cases} \qquad (15)$$

These piecewise linear reaction functions are displayed in Fig. 3 in white against a background of the profit surfaces for the first and second firms respectively, represented in terms of shading, the darker shade indicating higher profits. Due to the symmetry of the cases the pictures are rotations of each other with the diagonal as rotation axis.

In Fig. 4 we superpose the two reaction functions quite as Palander did. Equations (14)-(15) have two intersections, $x = y = 2000/3$ and $x = y = 2000$, obtained by either equating x' to y in (14) or y' to x in (15). As the slopes of the reaction functions (both pieces) are -1/2, both equilibria, the Cournot points, are locally stable. They hence coexist with each its proper basin of attraction in the space of initial conditions.

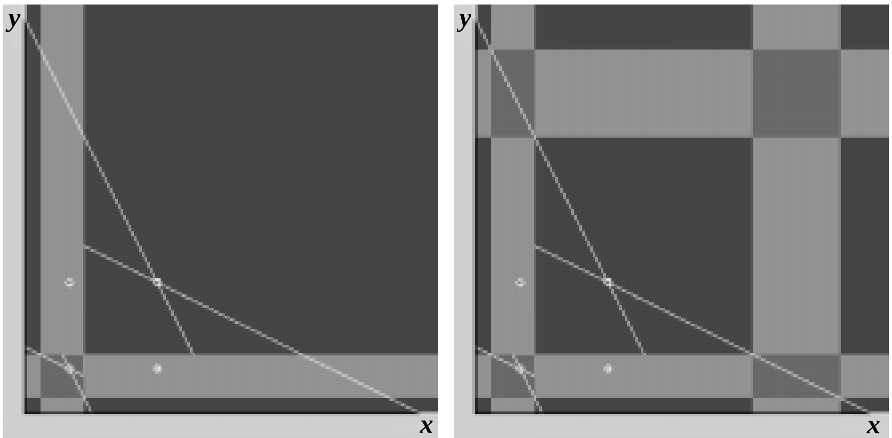

Fig. 4. Reaction functions and attraction basins according to Palander (left), and complete description (right). Ranges displayed for x and y: [0, 6500].

Note that the slopes of the reaction function always have this value, so all Cournot equilibria are stable. This is due to the linearity of the demand function. In all profit expressions the output of the optimising firms enters by its square, while that of the competitor enters linearly. By differentiation then, to get marginal revenue, as we see from (3)-(4), the competitor's sales enters with half the coefficient of the firm's own sales. So, this constantly low slope makes all the intersections of reaction functions into stable equilibrium points.

At least this is so with two competitors. We can note in passing that in the general case of n competitors, the Jacobian matrix has (n - 1) eigenvalues equal to 1/2 and 1 eigenvalue equal to -(n - 1)/2. Accordingly, with $n > 3$, the equilibrium points are no longer stable. For instance first explorative simulations indicate that with four competitors the first Palander case has an attractive 13-period cycle.

The left picture in Fig. 4 displays the attraction basins for the two coexistent fixed points exactly as described by Palander, and a basin from which the process was supposed to go to a 2-period oscillation.

To be quite exact, in discussing the dynamics of the iterated map $(x', y') = (\phi(y), \varphi(x))$ according to (14)-(15), Palander, like most authors of his day, was very keen on distinguishing between two different systems, respectively called "*simultaneous adjustment*", and "*alternative adjustment*". In the first case both competitors react on the actual supplies recorded from the previous period, in the latter they take turns in reacting. In terms of dynamics there is actually no difference. We can always compose two *inde-*

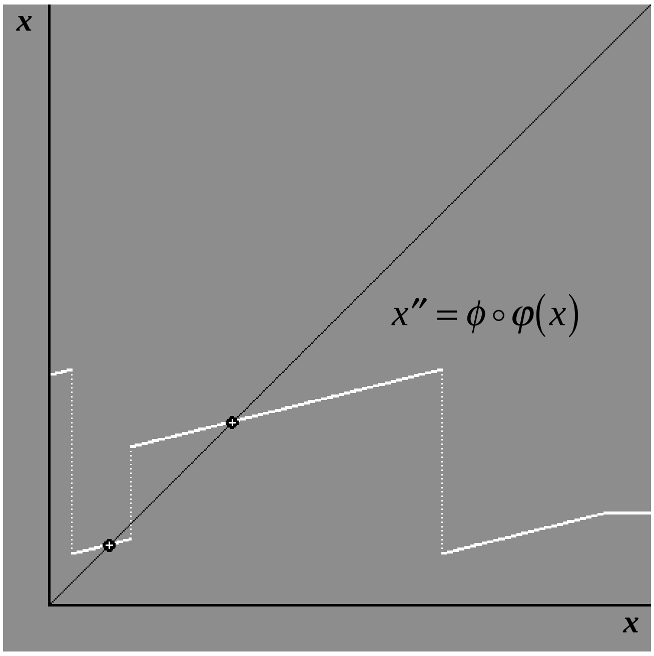

Fig. 5. Composite of reaction functions and diagonal. Range shown [0, 6500].

pendent iterations $x'' = \phi \circ \varphi(x)$ and $y'' = \varphi \circ \phi(y)$ *in each variable alone*, only note that the processes then run with a basic period twice as long as the one originally introduced. The dynamics is exactly *the same* in *both* of Palander's adjustment schemes. The only difference lies in the fact that, for the "alternative" case, the process cannot start out from every initial condition in *x*, *y* -space, the initial *y*-coordinate being a first iterate of the first *x*-coordinate, and vice versa. So, alternative adjustment just does not recover the full dynamics possibilities of Palander's model.

The composite iteration, which can be seen in Fig. 5, is:

$$x'' = \phi \circ \varphi(x) = \begin{cases} 2500 + x/4 & 0 < x < 400\sqrt{21} - 1600 \\ 500 + x/4 & 400\sqrt{21} - 1600 < x < 1800 - 200\sqrt{21} \\ 1500 + x/4 & 1800 - 200\sqrt{21} < x < 400\sqrt{21} + 2400 \\ -500 + x/4 & 400\sqrt{21} + 2400 < x < 6000 \\ 0 & 6000 < x \end{cases} \quad (16)$$

and, as mentioned, there is an identical expression for the composite $y'' = \varphi \circ \phi(y)$. The Cournot equilibria can also be recovered from (16) by equating x'' to x, though only from the second and third pieces because the ones obtained from the first and fourth are not in the intervals of relevance specified in the composite function. Put in other words, in Fig. 5 the relevant pieces of (16) do not intersect the diagonal.

To describe the basins, we define the two strips:

$$S_x = \left\{ (x, y) \middle| 400\sqrt{21} - 1600 < x < 1800 - 200\sqrt{21} \right\} \tag{17}$$

$$S_y = \left\{ (x, y) \middle| 400\sqrt{21} - 1600 < y < 1800 - 200\sqrt{21} \right\} \tag{18}$$

They are shown in the brightest shade in Fig. 4. The extrema defining the strips S_x and S_y are the first two discontinuity points of the composite reaction function (16) displayed in Fig. 5. For initial conditions $(x_0, y_0) \in S_x \cap S_y$, i.e. in the intersection of the two strips, the process goes to the lower Cournot equilibrium point. However, in a complete analysis, there are also initial points to the right of the third discontinuity point in (16), which also belong to the basin of the lower fixed point, as we will see below. For the moment, let us follow Palander's reasoning: For initial conditions in the union of the strips, net of the intersection, $(x_0, y_0) \in (S_x \cap S'_y) \cup (S'_x \cap S_y)$, the process goes to a 2-period oscillation, and for all other initial conditions it goes to the higher Cournot equilibrium. In all Palander described one quadratic basin for the lower equilibrium, four rectangular basin pieces for the higher equilibrium, and four rectangular basin pieces for oscillation, nine pieces in all.

Palander missed the full description of the basins, because he did not note that the various areas in his account also had preimages under the mapping. So, suppose we define two more strips:

$$T_x = \left\{ (x, y) \middle| 400\sqrt{21} + 2400 < x < 9200 - 800\sqrt{21} \right\} \tag{19}$$

$$T_y = \left\{ (x, y) \middle| 400\sqrt{21} + 2400 < y < 9200 - 800\sqrt{21} \right\} \tag{20}$$

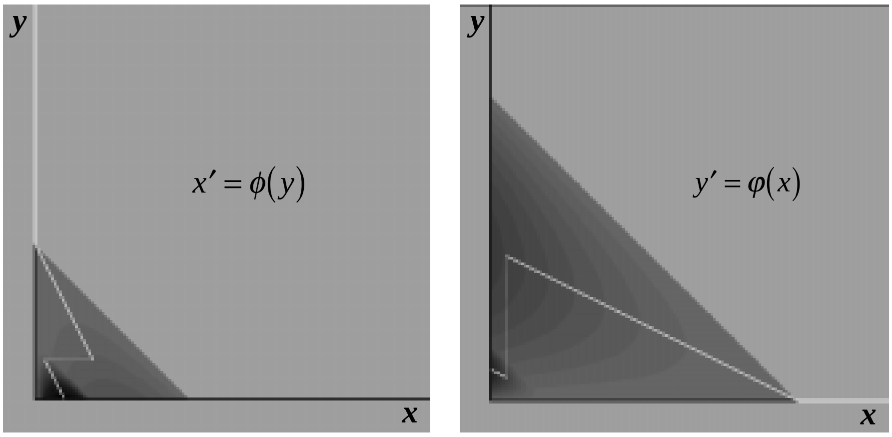

Fig. 6. Profit surfaces for the two firms in Palander's second case represented in terms of shading and the raction curves for the firms. Ranges for x,y: [0, 6500].

These strips are the new bright shade ones in the right picture of Fig. 4. Their intersections with the previous strips give rise to three new basin pieces for the lower Cournot equilibrium, further adding to and fragmenting the basins for the upper equilibrium and for oscillation so that the total number of pieces increases from 9 to 25. If it were not for the horizontal sections of the reaction functions, we could continue this process ad infinitum, but, in fact, it stops here. Note from Fig. 4 how the new strips (19)-(20) form by the intersections of the reaction functions with the old strips (17)-(18).

3 Palander's Second Case

As an alternative Palander, in his Swedish article, but not in the abstract, suggested:

$$p = f(q) = \begin{cases} 100 - \dfrac{q}{10} & q < 900 \\ \dfrac{500}{41} - \dfrac{q}{410} & q > 900 \end{cases} \tag{21}$$

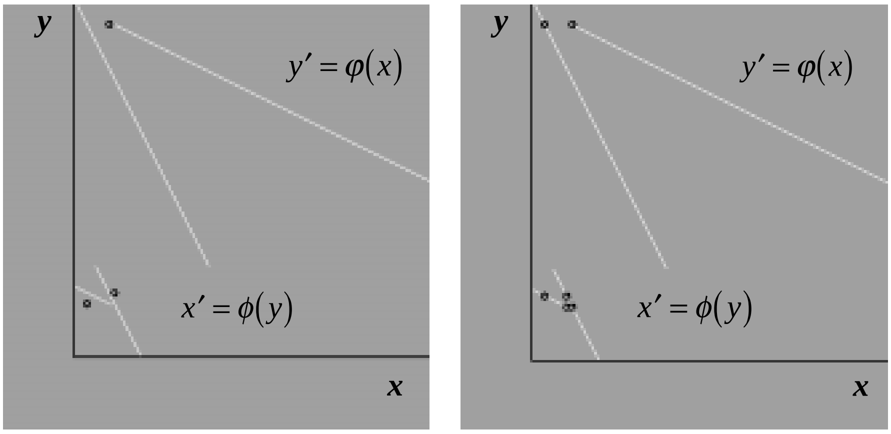

Fig. 7. Three-cycle for Palander's second case (left) and coexistent six-cycle (right). Ranges for x, y: [0, 3000].

where the first firm has a constant marginal = average cost equal to 6, whereas the second firm still has zero production cost. By exactly the same procedure as before, this time not forgetting to subtract costs from the revenues for the first firm, we obtain the reaction functions:

$$x' = \phi(y) = \begin{cases} 470 - \dfrac{y}{2} & 0 < y < 900 - 40\sqrt{41} \\ 1270 - \dfrac{y}{2} & 900 - 40\sqrt{41} < y < 2540 \\ 0 & 2540 < y \end{cases} \tag{22}$$

$$y' = \varphi(x) = \begin{cases} 500 - \dfrac{x}{2} & 0 < x < 900 - 100\sqrt{41} \\ 2500 - \dfrac{x}{2} & 900 - 100\sqrt{41} < y < 5000 \\ 0 & 5000 < y \end{cases} \tag{23}$$

They are displayed in Fig. 6, again against the background of the profit surfaces indicated by shading. It is easy to check that the reaction functions do

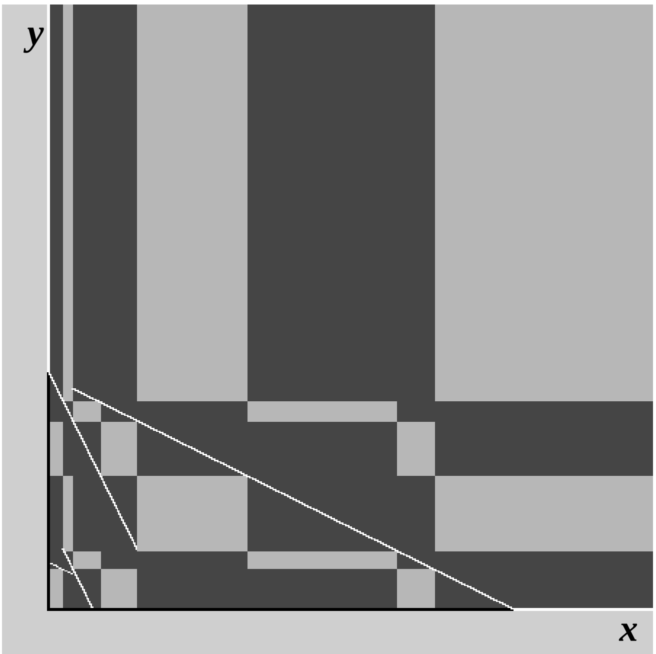

Fig. 8. The basins for the 3-cycle (*bright*) *and the 6-cycle* (*dark*). *Range for x and y:* [0, 6500]

not intersect, and so there exist no Cournot equilibria at all. Palander noted the existence of a stable 3-period cycle. See Fig. 7, the left picture. However, there is a coexistent 6-cycle, as we see in the right picture of Fig. 7, in a somewhat increased resolution in order to see all the points as distinct. The basin, shown in Fig. 8 is quite complex, as we see. Again the pattern would be repeated ad infinitum if we did not have the (white) vertical and horizontal segments of the reaction function, which are again due to the fact that supply cannot become negative.

In his picture for the second case, Palander showed a shaded area, without commenting its significance at all. He definitely did not designate it as a basin for the 3-period oscillation. In view of Fig. 8 it is, in fact, a mixture of the basins for the two coexistent oscillations. Probably he checked this area and noted that the system went to oscillatory motion, whereas he left the rest of the plane unchecked. The coexistence of the different cycles for a more general class of models has recently been established by Bischi, Mammana, and Gardini (2000).

It is interesting to note, in numerical simulations, though difficult to see in Fig. 7, that both in the 3-cycle and in the 6-cycle it is always the same three values for the *x*-coordinate and the *y*-coordinate, though different for the coordinates, which are visited. The way the 3-cycle becomes a 6-cycle is by each competitor lingering two periods at the same supply. As the time series for x and y are displaced, it then takes six periods to arrive at the same combination of coordinate values. It is also noteworthy that, whereas in the 3-cycle the points are not on the reaction curves, in the 6-cycle they in fact are. So, though assuming Palander's "simultaneous" adjustment, the process itself settles at "alternative" adjustment. See Table 1.

Table 1. Coordinates for 3-cycle and 6-cycle.

3-period cycle		6-period cycle	
x-coordinate	*y*-coordinate	*x*-coordinate	*y*-coordinate
280.6349	454.9206	280.6349	378.7302
242.5396	2359.6825	280.6349	2359.6825
90.1587	378.7302	90.1587	2359.6825
280.6349	454.9206	90.1587	454.9206
242.5396	2359.6825	242.5396	454.9206
90.1587	378.7302	242.5396	378.7302
280.6349	454.9206	280.6349	378.7302

4 Cubic Demand Functions

It is also interesting in this context to consider the case of a cubic demand curve, as considered by for instance Joan Robinson (1933), and hence also a cubic marginal revenue curve, especially as combined with the standard text-book case of a quadratic (U-shaped) marginal cost curve. We now only need one single expression to state price:

$$p = A - B(x+y) + C(x+y)^2 - D(x+y)^3 \tag{24}$$

Provided we choose all the coefficients positive and such that

$$8BD < 3C^2 < 9BD \tag{25}$$

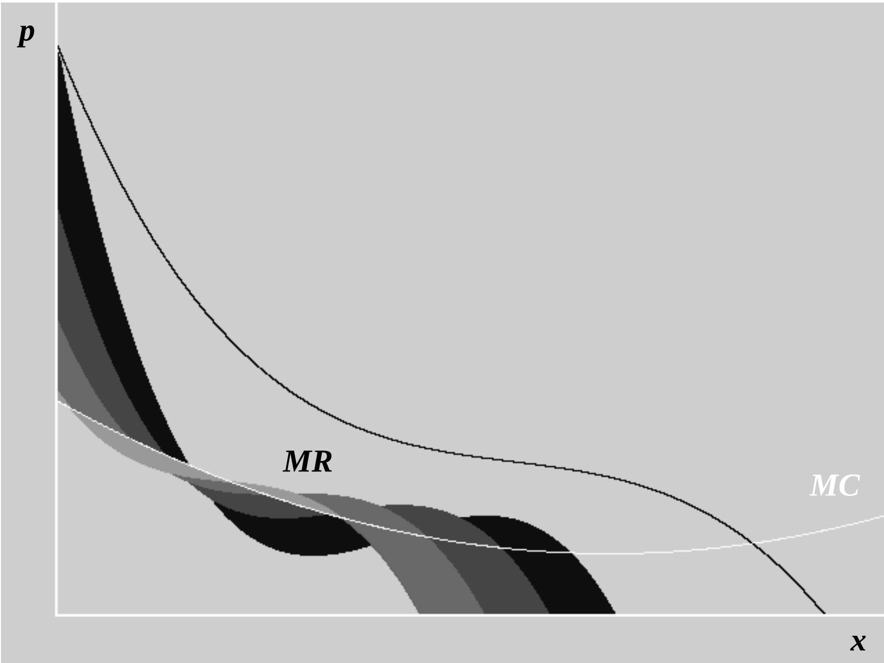

Fig. 9. Cubic demand, marginal cost, and marginal reveue curves for different supplies of the competitor. Range for x: [0, 7.5], *range for p:* [0, 6].

then the marginal revenue curve has a minimum followed by a maximum, while the demand curve is monotonically decreasing. Marginal revenues are obtained by multiplying (24) through by *x* for the first firm, by *y* for the second, and then differentiating with respect to that variable:

$$MR_x = \left(A - By + Cy^2 - Dy^3\right) - 2\left(B - 2Cy + 3Dy^2\right)x + 3(C - 3Dy)x^2 - 4Dx^3 \tag{26}$$

$$MR_y = \left(A - Bx + Cx^2 - Dx^3\right) - 2\left(B - 2Cx + 3Dx^2\right)y + 3(C - 3Dx)y^2 - 4Dy^3 \tag{27}$$

Supposing for simplicity the symmetrical case, so that the firms have identical, U-shaped marginal cost curves, we now write the marginal cost as:

$$MC_x = E - 2Fx + 3Gx^2 \tag{28}$$

$$MC_y = E - 2Fy + 3Gy^2 \tag{29}$$

Again all coefficients are positive, which gives the right kind of curvature, and we now require:

$$F^2 < 3EG \tag{30}$$

in order that in its minimum point marginal cost be still positive.

An example of suitable numerical coefficients are $A = 5.6$, $B = 2.7$, $C = 0.62$, $D = 0.05$, $E = 2.1$, $F = 0.3$, and $G = 0.02$. With these we have two local profit maxima, and now a profit minimum in between.

In Fig. 9 we display the situation quite as above in Fig. 1. Again, the darkest shade supports the marginal revenue function when the competitor supplies nothing, i.e. the firm is a monopolist. The more the competitor supplies the brighter the support shade. We can again compare the loss areas below the marginal cost curve with the gain areas above the marginal cost curve. It so seems that for the brightest shade, in the foreground, the loss outweighs the gain, and it also seems that the same holds true for the darkest shade, in the absolute background. Intermediate cases yield a larger gain area, which causes switching and reswitching. Fig. 10 displays the reaction functions $x' = \phi(y)$ and $y' = \varphi(x)$ for the two firms against a background of the profit surfaces, again in terms of shading. We see how they switch up from the lower local maximum to the upper, and reswitch back to the lower.

This classical textbook case would merit closer study, but it is computationally awkward. To get $x' = \phi(y)$ and $y' = \varphi(x)$ we have to solve the following cubic equations for local profit maxima, obtained through equating (26) to (28) and (27) to (29).

$$\begin{aligned}\left(A - E - By + Cy^2 - Dy^3\right) - 2\left(B - F - 2Cy + 3Dy^2\right)x'& \\ + 3\left(C - G - 3Dy\right)x'^2 - 4Dx'^3 = 0&\end{aligned} \tag{31}$$

$$\begin{aligned}\left(A - E - Bx + Cx^2 - Dx^3\right) - 2\left(B - F - 2Cx + 3Dx^2\right)y'& \\ + 3\left(C - G - 3Dx\right)y'^2 - 4Dy'^3 = 0&\end{aligned} \tag{32}$$

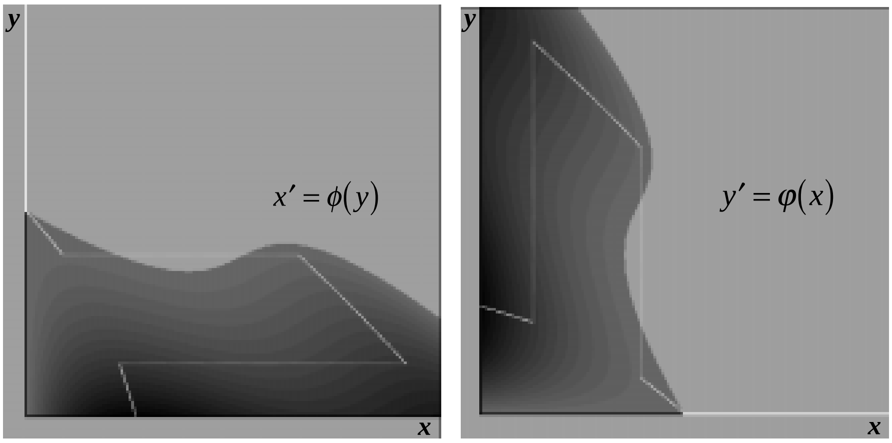

Fig. 10. Profit surfaces and reaction curves for the cubic demand case. Range shown for x and y: [0, 4.5].

Being third order equations, (31) and (32) may have three real roots for x' and y' respectively, which is the really interesting case. Then the intermediate root is a profit minimum, whereas the smallest and the largest provide local profit maxima. To decide between them it must be determined which is the global maximum, by evaluating the relevant quartic profit function:

$$\Pi_x(x', y) = \left(A - B(x'+y) + C(x'+y)^2 - D(x'+y)^3 - E + Fx' - Gx'^2\right)x' \quad (33)$$

$$\Pi_y(x, y') = \left(A - B(x+y') + C(x+y')^2 - D(x+y')^3 - E + Fy' - Gy'^2\right)y' \quad (34)$$

As we see in Fig. 10, we get nonlinear decreasing reaction curves with one switch up and another reswitch down. The lower segments in each picture are part of one single curve, representing the lower local profit maximum. Between this and the upper curve segment there is a locus for the minima, not drawn in the pictures, but with a position which can be inferred from the shading.

Equating $x = x'$ and $y = y'$, subtracting (31) from (32), and factoring, we get the equation:

$$(x-y)\left(3D(x+y)^2 - (2C-3G)(x+y) + B - 2F\right) = 0 \quad (35)$$

for the location of possible Cournot equilibria. The first factor yields $x = y$, which substituted into (31) and (32), yields:

$$(A-E)-(3B-2F)x+(8C-3G)x^2-20Dx^3=0 \tag{36}$$

$$(A-E)-(3B-2F)y+(8C-3G)y^2-20Dy^3=0 \tag{37}$$

The three roots, possible Cournot equilibria, are two intersections between the profit maximising branches or the reaction functions, and one between the minimising, though one or both of the former may, but need not in general, be excluded by the jump conditions.

From (31) and (32) we can also (by implicit differentiation) obtain the slopes of the reaction functions in the Cournot points (where as we remember $x = y$):

$$\frac{dx'}{dy}=-\frac{B-6Cy+24Dy^2}{2B-2F-(10C-6G)y+36Dy^2} \tag{38}$$

$$\frac{dy'}{dx}=-\frac{B-6Cx+24Dx^2}{2B-2F-(10C-6G)x+36Dx^2} \tag{39}$$

If they multiply to a value larger than unity, then the Cournot equilibria lose stability and there is a possibility for complex dynamics. To judge from our numerical case, illustrated in Fig. 10, the slopes might be sufficiently high. However, the reaction curves do not intersect at all, so we are in a case similar to Palander's second. Provided we skip the simplifying assumption of identical firms, things become even more complicated.

It is better to try things out through linear approximation, replacing the falling branch of the marginal cost curve with a straight line and letting the kinked linear demand curve replace the qualitatively similar cubic. As we will find things become interesting enough.

5 Decreasing Marginal Cost

So, let us revert to the kinked demand curve case as suggested by Palander, and assume:

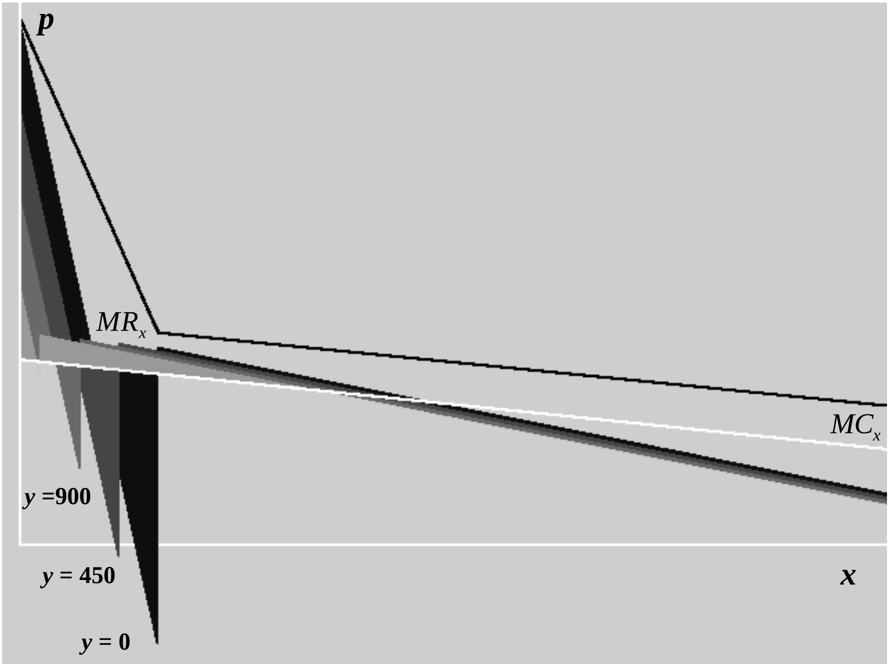

Fig. 11. Demand, falling marginal cost, and marginal reveue curves for different supplies of the competitor. Range for x: [0, 10000], *range for p:* [0, 155].

$$p = f(x+y) = \begin{cases} \alpha_1 - \beta_1(x+y) & x+y \le \bar{q} \\ \alpha_2 - \beta_2(x+y) & x+y > \bar{q} \end{cases} \tag{40}$$

where

$$\bar{q} = \frac{\alpha_1 - \alpha_2}{\beta_1 - \beta_2} \tag{41}$$

is the quantity coordinate at the kink point. Note that to have the right kind of kink we must have $\alpha_1 > \alpha_2$, $\beta_1 > \beta_2$. Given we take $\alpha_1 = 150$, $\alpha_2 = 450/7$, $\beta_1 = 0.0565$ and $\beta_2 = 0.00249$, this indeed is the case. The facts are illustrated in Fig. 11, We see the kinked demand curve, familiar by now from the original Palander cases, and further a selection of marginal revenue curves, drawn at regular intervals of the supply for the competitor 0, 450, 900, and 1350. As usual the darker shade represents a smaller supply by the competitor, the darkest being the case of a monopolist.

Further suppose we have quadratic total cost functions, i.e. linear marginal cost functions:

$$C_x = g_x(x) = a_x x - b_x x^2 \tag{42}$$

$$C_y = g_y(y) = a_y y - b_y y^2 \tag{43}$$

In general we take a_x, b_x, a_y, b_y positive to have down sloping marginal cost curves. In particular take the numerical coefficients $a_x = a_y = 53$ and $b_x = 1/780$ and $b_y = 1/800$. The marginal cost curves hence have the same intercept, 53, whereas the slopes, 1/390 and 1/400, are very slightly different. Fig. 11 was drawn for the first firm, but the difference is so slight that it would almost be imperceptible in the picture. As we see, though the marginal cost curves are down sloping, we took care that the firms never operate in the region where there is in any danger for marginal costs becoming negative. Again we can, by comparing loss and gain areas, see that in the case of virtual monopoly, $y = 0$, the first firm would choose the lower intersection of the marginal cost and revenue curves, whereas for $y = 1350$ it would definitely choose the higher one, as there is hardly any loss area at all.

From (40) and (42)-(43) we now get profits:

$$\Pi_x = f(x+y)x - g_x(x) \tag{44}$$

$$\Pi_y = f(x+y)y - g_y(y) \tag{45}$$

The pieces of the reaction functions for the first firm are obtained by differentiating profits (44) with respect to x, equating to zero, and solving, equivalent to the procedure of equating marginal revenue to marginal cost. We get two solutions:

$$x' = \frac{1}{2}\frac{\alpha_1 - a_x}{\beta_1 - b_x} - \frac{y}{2}\frac{\beta_1}{\beta_1 - b_x} \qquad x' = \frac{1}{2}\frac{\alpha_2 - a_x}{\beta_2 - b_x} - \frac{y}{2}\frac{\beta_2}{\beta_2 - b_x} \tag{46}$$

As usual these are results of local optimization. The choice of branch is due to globally maximal profits. Substituting from the reaction curve branches in

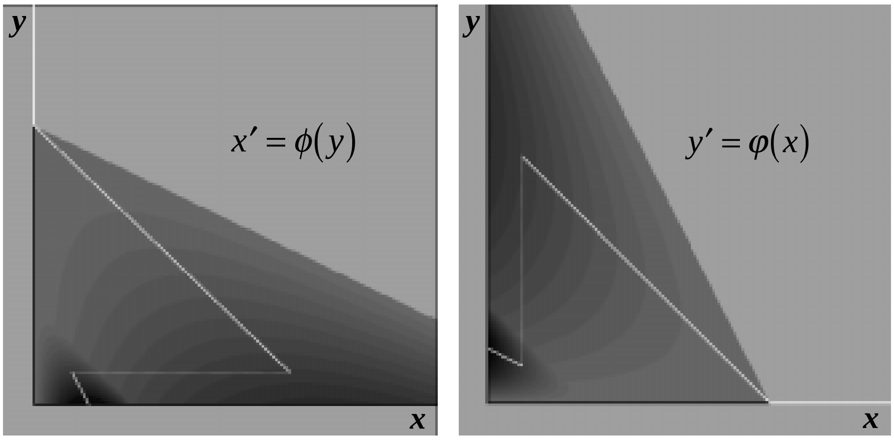

Fig. 12. Profit surfaces and reaction curves for the decreasing linear marginal cost case. Ranges shown for x and y: [0, 6500].

the profit expression (44) we get local maximum profits for the first firm as dependent on the supply of the competitor alone:

$$\Pi_x^1 = \frac{(\alpha_1 - a_x - \beta_1 y)^2}{4(\beta_1 - b_x)} \qquad \Pi_x^2 = \frac{(\alpha_2 - a_x - \beta_2 y)^2}{4(\beta_2 - b_x)} \tag{47}$$

The procedure now runs as in Section 2, by establishing the ranges of validity for the branches, by substituting the reaction function pieces (46) in the condition for the choice of branch, according to (40) and (41), and considering that no supply quantity can be negative. In this way we find, this time skipping details, that again only one of the roots in the quadratic for y, obtained from equating the two expressions (47), is in the range where both branches are relevant. This root is:

$$\bar{y} = \frac{\alpha_1\sqrt{\beta_2 - b_x} - \alpha_2\sqrt{\beta_1 - b_x} - a_x\left(\sqrt{\beta_2 - b_x} - \sqrt{\beta_1 - b_x}\right)}{\beta_1\sqrt{\beta_2 - b_x} - \beta_2\sqrt{\beta_1 - b_x}} \tag{48}$$

and we can state the reaction function for the first firm as:

$$x' = \phi(y) = \begin{cases} \dfrac{1}{2}\dfrac{\alpha_1 - a_x}{\beta_1 - b_x} - \dfrac{y}{2}\dfrac{\beta_1}{\beta_1 - b_x} & 0 < y < \bar{y} \\ \dfrac{1}{2}\dfrac{\alpha_2 - a_x}{\beta_2 - b_x} - \dfrac{y}{2}\dfrac{\beta_2}{\beta_2 - b_x} & \bar{y} < y < \dfrac{\alpha_2 - a_x}{\beta_2} \\ 0 & \dfrac{\alpha_2 - a_x}{\beta_2} < y \end{cases} \tag{49}$$

Likewise, we obtain for the second firm:

$$y' = \varphi(x) = \begin{cases} \dfrac{1}{2}\dfrac{\alpha_1 - a_y}{\beta_1 - b_y} - \dfrac{x}{2}\dfrac{\beta_1}{\beta_1 - b_y} & 0 < x < \bar{x} \\ \dfrac{1}{2}\dfrac{\alpha_2 - a_y}{\beta_2 - b_y} - \dfrac{x}{2}\dfrac{\beta_2}{\beta_2 - b_y} & \bar{x} < x < \dfrac{\alpha_2 - a_y}{\beta_2} \\ 0 & \dfrac{\alpha_2 - a_y}{\beta_2} < x \end{cases} \tag{50}$$

with

$$\bar{x} = \frac{\alpha_1\sqrt{\beta_2 - b_y} - \alpha_2\sqrt{\beta_1 - b_y} - a_y\left(\sqrt{\beta_2 - b_y} - \sqrt{\beta_1 - b_y}\right)}{\beta_1\sqrt{\beta_2 - b_y} - \beta_2\sqrt{\beta_1 - b_y}} \tag{51}$$

We do not replicate the derivation, all the arguments run as before, just interchange *x* and *y* everywhere in the formulas (41)-(43).

The facts are illustrated in Fig. 12, where we as usual display the profit surfaces in terms of shading, according to (44) and (45). We also see the reaction functions.

The big difference now is that the slopes of some pieces of the reaction functions exceed unity and hence destabilise any Cournot equilibrium, provided it exists. Actually, as we may see in Fig. 13, there is no such equilibrium in the example, but the case nevertheless involves more complex dynamics than encountered up to now. It is a bit difficult, in this resolution, to see that the long almost concurrent reaction curve segments do not intersect, but they do not.

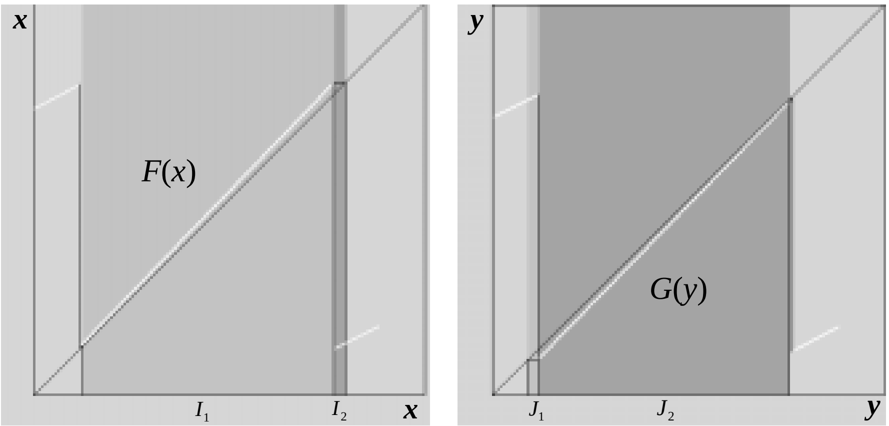

Fig. 13. Composite reaction functions. Range for x, y: [0, 5000]

Using the numerical specifications, we find the two slopes in equation (49) equal to $-\beta_1/2/(\beta_1 - b_x) \approx -0.5116$ and $-\beta_2/2/(\beta_2 - b_x) \approx -1.0307$, those in (50) to $-\beta_1/2/(\beta_1 - b_y) \approx -0.5113$ and $-\beta_2/2/(\beta_2 - b_y) \approx -1.004$. As already seen in the previous examples, the dynamics of the duopoly are strictly related to the dynamics of the one dimensional maps obtained as composite functions.

The graph of $x'' = \phi \circ \varphi(x) = F(x)$ is shown in Fig. 13 (left) and we see that the map is absorbing in the interval $I = I_1 \cup I_2$ because any initial condition is mapped by *F* into *I*, and *I* is invariant, *F*(*I*) = *I*. Moreover, it is easy to see that the dynamics of *F* are completely chaotic in the interval *I*. In fact, the function *F* in *I* is made up of two linear pieces: an expansion in I_1 with slope (-1.004)(-1.0307) = 1.034828, and a contraction in I_2, with slope (-1.004)(-0.5116) = 0.5136464. Then, as *F* is an expansion in I_1, any cycle of *F* in *I* must have at least one point in the interval I_2, but then any point $x_0 \in I_2$ is mapped by *F* in I_1: $x_1 = F(x_0) \in I_1$, and the expanding process starts. The number of iterations which are necessary in order to again get a point in the interval I_2 is higher than 21 (actually more than 50). As $(0.5136464)(1.034828)^{21} > 1$, we can conclude that the multiplier associated with any cycle of *F* in *I* is higher than 1, and all the cycles are thus unstable.

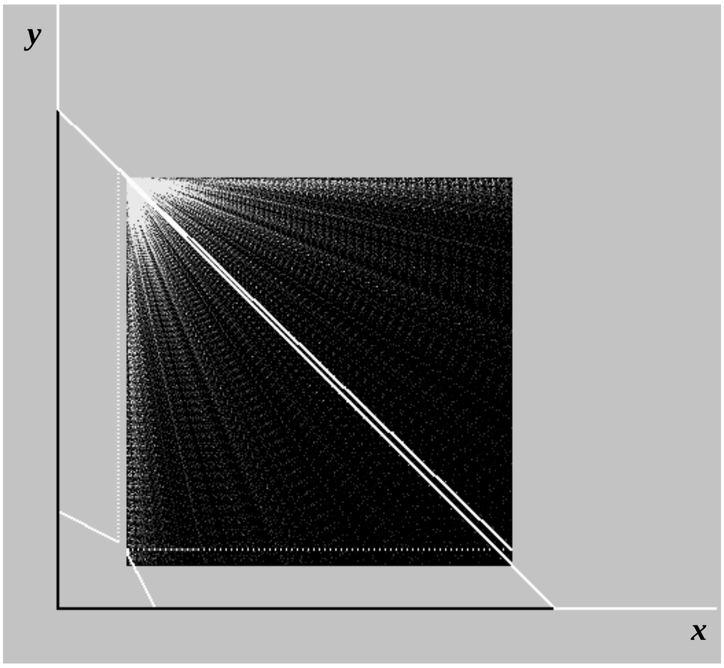

Fig. 14.Reaction functions in case of decreasing marginal costs and chaotic attractor. Range for x and y: [0, 6000].

As F is invariant in I we conclude that any initial condition is either asymptotically periodic to a repelling cycle or aperiodic, and thus F is chaotic in I. Similarly, $y'' = \varphi \circ \phi(y) = G(y)$, the graph of which is shown in Fig.13 (right), is absorbing and invariant in the interval $J = J_1 \cup J_2$, and it too is chaotic in that interval.

Summing up, for the dynamics of this duopoly game, whose double iterate is governed by the two maps F and G, we find that the rectangle $I \times J$ (the cartesian product) is absorbing and invariant in the phase space $\Re^2$ and that the dynamics are chaotic in $I \times J$. An example is shown in Fig.14. Note that from Fig. 13 we can deduce that all the trajectories spend more time (more iterations) in the lower part of the interval I and the upper part of interval J where the graphs of F and G are close to the diagonal. As a consequence the dynamics of the duopoly game visit the upper left corner of the rectangle $I \times J$ most frequently. This is shown in Fig. 14 where we used a colouring process: the brightness of shade represents the frequency of visiting in the iteration process. More on this kind of dynamics can be found in Chapter 7.

6 Wald's Second Model

As mentioned Abraham Wald suggested two cases where the kink in a piecewise linear demand function was replaced by a curve segment which smoothly and tangentially joined the line segments. The most interesting is the second example with the demand function:

$$p = g(x+y) = \begin{cases} 3 - 2(x+y) & x+y \le 1 \\ \dfrac{1}{(x+y)^2} & 1 \le x+y \le 4 \\ \dfrac{3}{16} - \dfrac{x+y}{32} & x+y \ge 4 \end{cases} \tag{52}$$

and zero marginal cost for both firms. To construct the reaction functions, profits (=revenues) according to the various expressions (52) are maximised. For the first firm we have the profits: $(3-2(x+y))x$, $x/(x+y)^2$, and $(6-(x+y))x/32$ respectively, and maximise with respect to *x*. In this way the reaction function branches:

$$x = \frac{3}{4} - \frac{y}{2} \tag{53}$$

$$x = y \tag{54}$$

$$x = 3 - \frac{y}{2} \tag{55}$$

are obtained. Wald does not need to compare profits for the various branches, it just suffices to consider the validity due to the inequality constraints in (52). Take the constraint $x+y \le 1$, substitute from (53), and solve for $y \le 1/2$. Likewise, take $1 \le x+y \le 4$, substitute from (54) and solve for $1/2 \le y \le 2$. Finally, take $x+y \ge 4$, substitute from (55), and solve for $y \ge 2$. As we see the three reaction curve pieces have exclusive ranges of relevance, so there are only two points, $y = 1/2$ and $y = 2$, in which the ranges meet.

The three local maximum profit expressions are easily calculated as $(3-2y)^2/6$, $1/(4y)$, and $(6-y)^2/128$ respectively, so in the points $y = 1/2$ and $y = 2$ profits are pairwise the same for the expressions, 1/2 and 1/8 respectively. So, unlike Palander, Wald does not need to compare profits for selecting a global optimum. The ranges of relevance are sufficient.

Considering also that no supply quantity can be negative, we add a lower bound for the first section and an upper bound in the third, and can so piece the reaction function for the first firm together:

$$x' = \phi(y) = \begin{cases} 3/4 - y/2 & 0 \le y \le 1/2 \\ y & 1/2 \le y \le 2 \\ 3 - y/2 & 2 \le y \le 6 \\ 0 & 6 \le y \end{cases} \tag{56}$$

and a similar one for the second firm:

$$y' = \varphi(x) = \begin{cases} 3/4 - x/2 & 0 \le x \le 1/2 \\ x & 1/2 \le x \le 2 \\ 3 - x/2 & 2 \le x \le 6 \\ 0 & 6 \le x \end{cases} \tag{57}$$

As we see the reaction functions coincide along the entire middle segment, so, as Wald noted, there is a continuum of Nash equilibria $x = y$ along the entire line segment.

Considering the dynamics, which Wald did not, it is easy to see from the definition of the reaction functions $y' = \varphi(x)$ and $x' = \phi(y)$ that, given any initial condition (x_0, y_0) with $x_0 > 0$ and $y_0 > 0$, in one or at most two iterations $y_1 = \varphi(x_0)$ or $x_2 = \phi(y_1)$ jumps into the interval [0.5, 2], and $x_1 = \phi(y_0)$ or $y_2 = \varphi(x_1)$ as well into the interval [0.5, 2]. Thus any further iterations remain confined inside the square $S = [0.5, 2] \times [0.5, 2]$ of the phase plane. In fact, either $x_2 = y_2$, so we arrive at a fixed point. Or $x_2 \ne y_2$, so we are in a cycle of period two: (x_0, y_0), (x_1, y_1), (x_2, y_2), (y_2, x_2), (x_2, y_2)...

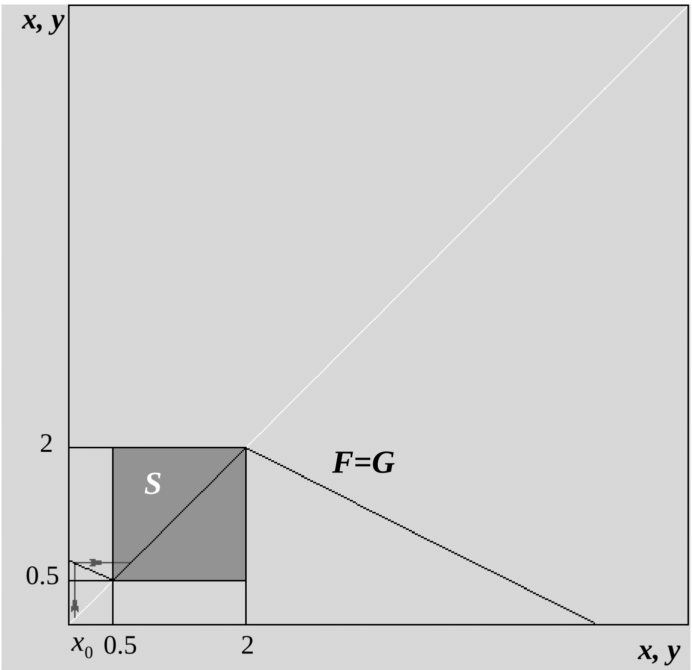

Fig. 15. Composite Wald reaction functions F(x) and G(y), (identical). Variable ranges [0, 7].

Thus all the points on the diagonal of *S*, (*x*, *x*) with $0.5 \le x \le 2$, are infinitely many (uncountable) fixed points of the game, while all the points in *S* off the diagonal, say (x, y), with $x \ne y$ and $x, y \in [0.5, 2]$, belong to infinitely many (uncountable) cycles of period two $((x, y), (y, x), (x, y), \ldots)$. Note also that all the fixed points are stable but not asymptotically stable, as any initial condition in a neighbourhood of a fixed point (*x*, *x*) will not give rise to a sequence converging to that fixed point, but either to a two-cycle or to a different fixed point in a neighbourhood of (*x*, *x*). Similarly, for the same arguments, all the two-cycles are stable but not asymptotically stable. As there are infinitely many such oscillations and basins for them, there is no point in drawing basin pictures. This type of coexistence has a strong flavour of structural instability.

Unfortunately, we cannot remove the symmetry of the firms from Wald's model, because any nonzero cost (the only characterising difference between the competitors) would cause us to have to solve a third degree equation for getting the reaction function for the middle piece. If so, we could as well go back to the cubic case treated above.

Accordingly the Palander examples are much more useful to elaborate than the Wald cases.

7 A Modified Wald Model

Departing from Wald's second example we may construct a simpler demand function, where the middle segment is just a hyperbola replaced by tangent straight lines at the ends, say:

$$p = \begin{cases} 4 - 4q & q \le 0.5 \\ 1/q & 0.5 \le q \le 2 \\ 1 - q/4 & q \ge 2 \end{cases} \tag{58}$$

The original Wald cases must be regarded as mere examples, without any subject matter significance. The hyperbola, $p = 1/q$, however, arises in a natural way in basic economic models. For instance, whenever the utility functions of the consumers have Cobb-Douglas shape, then utility maximisation results in constant budget shares for each commodity. Constant budget shares, however, mean that demand of each commodity is reciprocal to its price. As this holds for all consumers, this is one of the rare cases where the aggregation problems are easily solved, and aggregate demand as well becomes reciprocal to price.

There is a problem with this type of demand function. When used as demand function for a monopolist, the result is no definite profit maximum. This is because price times quantity sold, i.e. total revenue, is independent of price. By letting price become infinite and the quantity go to zero the monopolist can retain the same constant revenue, but cut any production costs down to zero. This, of course, is a symptom of something basically wrong in the assumptions. In no consumption theory does it make sense to buy zero fractions of units of a commodity at infinite prices. The function (58) is one way of dealing with this problem. (In another chapter we deal with this by adding a positive constant in the denominator instead.)

Now, dealing with duopolists having constant marginal costs c_x, c_y, we obtain the reaction functions:

$$x' = \phi(y) = \begin{cases} (4 - c_x)/8 - y/2 & 0 < y < c_x/4 \\ \sqrt{y/c_x} - y & c_x/4 < y < 4c_x \\ 2(1 - c_x) - y/2 & 4c_x < y < 4(1 - c_x) \\ 0 & 4(1 - c_x) < y \end{cases} \quad (59)$$

$$y' = \varphi(x) = \begin{cases} (4 - c_y)/8 - x/2 & 0 < x < c_y/4 \\ \sqrt{y/c_y} - x & c_y/4 < x < 4c_y \\ 2(1 - c_y) - x/2 & 4c_y < x < 4(1 - c_y) \\ 0 & 4(1 - c_y) < x \end{cases} \quad (60)$$

These are similar to Wald's original reaction functions, but in the middle section the straight line is replaced by a curve segment. Further, we may now introduce an asymmetry between the firms (different c_x, c_y), as it is possible to solve for the middle sections of the reaction functions in closed form even with nonzero costs.

Let us fix the parameter c_y = 0.53 and study what happens as we successively decrease the parameter c_x, from c_x = 0.1. At c_x = 0.1, the two composite functions $x'' = \phi \circ \varphi(x) = F(x)$ and $y'' = \varphi \circ \phi(y) = G(y)$ have a globally stable fixed point. Thus also the duopoly game has only one globally stable fixed point. Put $F(x^*) = x^*$. Then, defining $y^* = \varphi(x^*)$, we have $G(y^*) = y^*$. From $F(x^*) = \phi \circ \varphi(x^*) = x^*$ we deduce that $\phi(y^*) = x^*$, so $G(y^*) = \varphi \circ \phi(y^*) = \varphi(x^*) = y^*$. Then (x^*, y^*) is the only fixed point of our map.

However, as c_x decreases, the fixed point becomes repelling and the two composite functions both get an attracting cycle of period 2 (see Fig. 16 drawn for c_x = 0.05). Let x_1 and x_2 be the two points of the cycle of *F*, and define $y_1 = \varphi(x_1)$ and $y_2 = \varphi(x_2)$. Then we see that y_1 and y_2 are the periodic points of *G*. In fact, as $\phi \circ \varphi(x_1) = F(x_1) = x_2$ we deduce that $\phi(y_1) = x_2$,

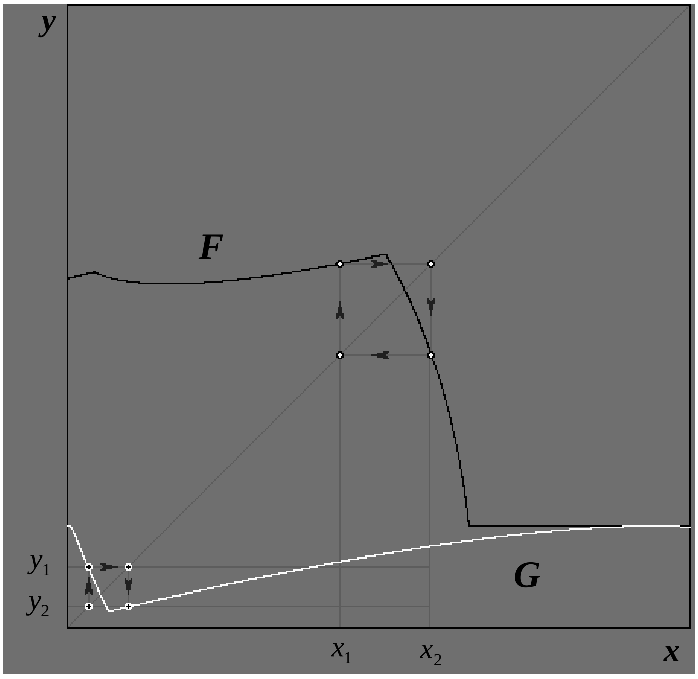

Fig. 16. Composite reaction functions and 4-cycle. Variable range [0, 3].

and as $\phi \circ \varphi(x_2) = F(x_2) = x_1$ we deduce that $\phi(y_2) = x_1$. Then we have $G(y_1) = \varphi \circ \phi(y_1) = \varphi(x_2) = y_2$ and similarly $G(y_2) = \varphi \circ \phi(y_2) = \varphi(x_1) = y_1$. As these two cycles are globally attracting for the composite functions we can deduce that the duopoly game *T* has a unique attractor which is a cycle of period 4. The point (x_1, y_1) is mapped by *T* in the following sequence:

$$\begin{aligned} (x_1, y_1) \quad &\to T \to (\phi(y_1), \varphi(x_1)) = (x_2, y_1) \\ &\to T \to (\phi(y_1), \varphi(x_2)) = (x_2, y_2) \\ &\to T \to (\phi(y_2), \varphi(x_2)) = (x_1, y_2) \\ &\to T \to (\phi(y_2), \varphi(x_1)) = (x_1, y_1) \end{aligned} \tag{61}$$

Besides the repelling fixed point (x^*, y^*) of the map *T*, we also have another repelling cycle of period four, in fact, all the periodic points of the map *T*

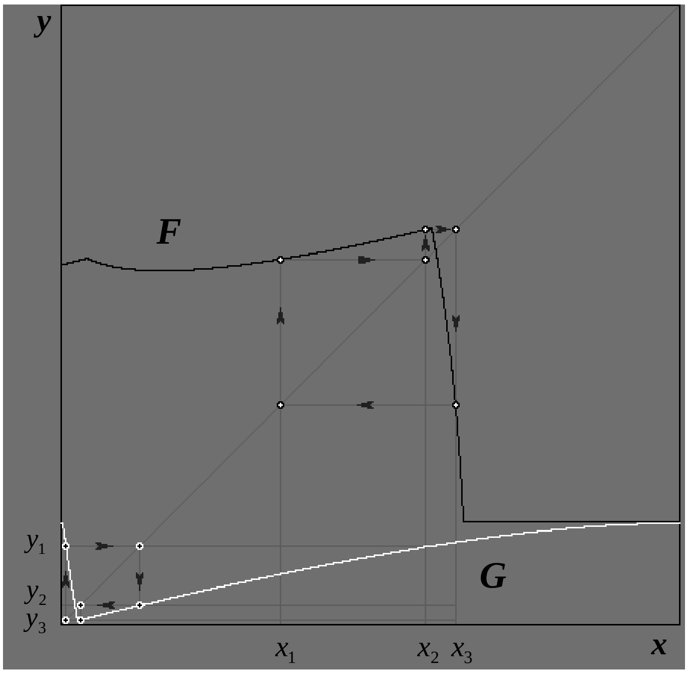

Fig. 17. Composite reaction functions, 3- and 6-cycles. Variable range [0, 3].

belong to the Cartesian product $\{x_1, x_2, x^*\} \times \{y_1, y_2, y^*\}$ and besides the stable 4-cycle and the fixed point (repelling node) we also have a saddle cycle of period 4:

$$\begin{aligned}(x^*, y_1) \quad &\to T \to (\phi(y_1), \varphi(x^*)) = (x_2, y^*) \\ &\to T \to (\phi(y^*), \varphi(x_2)) = (x^*, y_2) \\ &\to T \to (\phi(y_2), \varphi(x^*)) = (x_1, y^*) \\ &\to T \to (\phi(y^*), \varphi(x_1)) = (x^*, y_1)\end{aligned} \tag{62}$$

It is easy to predict that as c_x is further decreased, more complex dynamics may occur, including bistability.

As an example we see that at c_x = 0.02 the composite functions have an attracting cycle of period three, see Fig. 17 Let $\{x_1, x_2, x_3\}$ be the 3-cycle of F (with $x_{i+1} = F(x_i)$, see Fig. 17), and define $y_i = \varphi(x_i)$ for i= 1, 2, 3. Then

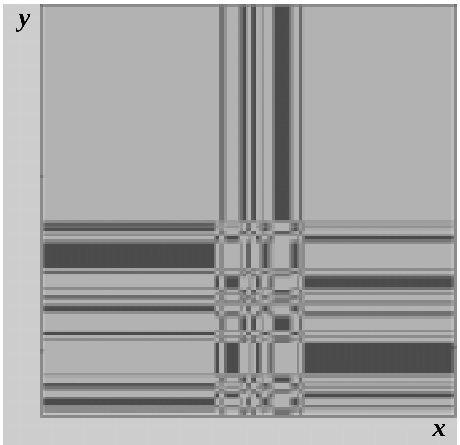

Fig. 18. Basins for coexistent 3- and 6-cycles. Axes: x, y in interval [0, 3].

we have $\phi(y_1) = x_2$, $\phi(y_2) = x_3$, $\phi(y_3) = x_1$, hence $G(y_1) = y_2$, $G(y_2) = y_3$, $G(y_3) = y_1$. It follows that the cartesian product $\{x_1, x_2, x_3\} \times \{y_1, y_2, y_3\}$ includes stable periodic points. We have:

$$
\begin{aligned}
(x_1, y_1) \quad & \to T \to (\phi(y_1), \varphi(x_1)) \to (x_2, y_1) \\
& \to T \to (\phi(y_1), \varphi(x_2)) \to (x_2, y_2) \\
& \to T \to (\phi(y_2), \varphi(x_2)) \to (x_3, y_2) \\
& \to T \to (\phi(y_2), \varphi(x_3)) \to (x_3, y_3) \\
& \to T \to (\phi(y_3), \varphi(x_3)) \to (x_1, y_3) \\
& \to T \to (\phi(y_3), \varphi(x_1)) \to (x_1, y_1)
\end{aligned}
\tag{63}
$$

which is a 6-cycle of T, whose points are clearly visible in Fig. 17 But there is also an attracting 3-cycle:

$$
\begin{aligned}
(x_1, y_2) \quad & \to T \to (\phi(y_2), \varphi(x_1)) \to (x_3, y_1) \\
& \to T \to (\phi(y_1), \varphi(x_3)) \to (x_2, y_3) \\
& \to T \to (\phi(y_3), \varphi(x\ )) \to (x_1, y_2)
\end{aligned}
\tag{64}
$$

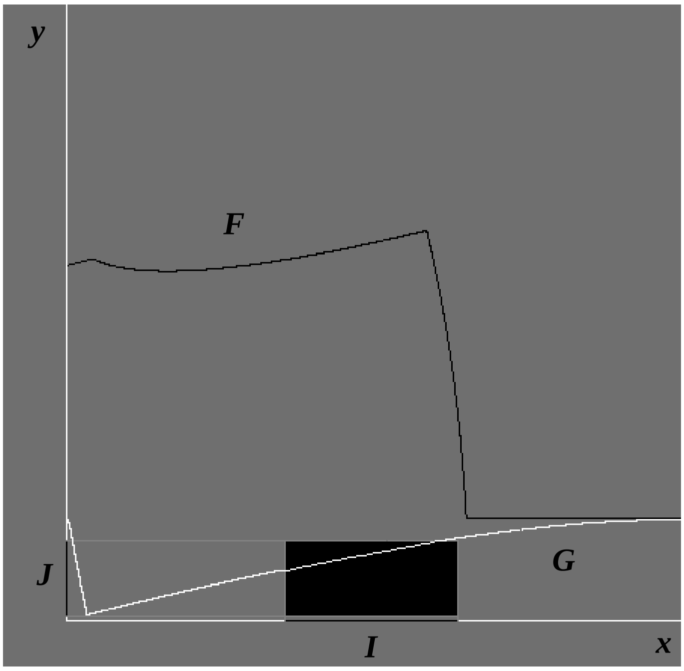

Fig. 19. Chaotic attractor in 1 piece. Axes intervals: x, y: [0, 3].

Further, note that the cartesian product $\{x_1, x_2, x_3, x^*\} \times \{y_1, y_2, y_3, y^*\}$ includes periodic points, and besides the two cycles given above we have the repelling fixed point and the repelling cycle of period 6 of saddle type given by $(x^*, y_1)\ldots$ The stable set of this saddle of period 6, which is made up of vertical and horizontal lines issuing from the periodic points and their preimages, as shown by Bischi, Mammana, and Gardini (2000), separating the two basins of attraction of the map *T*, as shown in Fig. 18, where the light grey points belong to the basin of the 6-cycle while the dark-grey points constitute the basin of the 3-cycle.

We note however that the basins shown in Fig. 18 are only approximate, and the picture is a consequence of the numerical impossibility to see the fine structure of repelling Cantor sets. For example it includes also the repelling fixed point in some rectangle but it is clear that it is a repellor and that point will not converge to any other cycle. Similarly we have infinitely many other cycles existing in the phase plane, all unstable, and such points, together with their stable sets, cannot be seen in the figures numerically computed, but their existence can be rigorously proved.

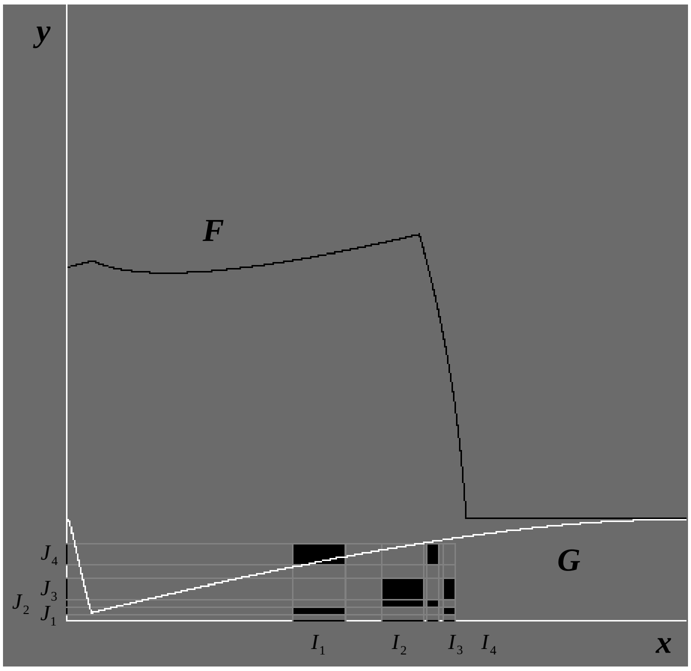

Fig. 20. Chaotic attractor in 8 pieces. Axes intervals: x, y: [0, 3].

Note the great difference in comparison to the case considered in Section 3, where the basins shown in Fig. 8 too were associated with cycles of period 3 and 6 of the map. In that example the composite functions *F* and *G* were *discontinuous*, and all pieces constituting *F* and *G* had slope 1/4, so that the 3-cycle $\{x_1, x_2, x_3\}$ of *F* was its only cycle (globally attracting), and similarly for *G*. The map *T* can only have those two stable cycles, whose periodic points belong to the cartesian product $\{x_1, x_2, x_3\} \times \{y_1, y_2, y_3\}$, and their basins are separated by the lines in which the discontinuous map changes by definition, and of their preimages.

Differently, in the case shown in Fig. 17, the reaction functions are *continuous*, so that the maps *F* and *G* are continuous too, and the Sharkovsky theorem applies, which means that *F* and *G* possess infinitely many repelling cycles of any order. It also follows that the map *T* has infinitely many repelling cycles of any order as the cartesian product of (periodic points of F)$\times$(periodic points of G) includes all periodic points of the map *T.* See the proof in Bischi, Mammana, and Gardini (2000).

It is easy to deduce that, as the parameter c_x decreases from 0.05 to 0.02, chaotic dynamics in *F* and *G* occur, so that also chaotic dynamics of *T* exist. An example is shown in Fig. 19 (c_x = 0.025), where *F* is chaotic on an interval *I*, *G* is chaotic on the interval $J = \varphi(I)$, and thus the map *T* is chaotic in the rectangle $I \times J$. Another example is shown in Fig. 20 (c_x = 0.0295) where *F* has 4-cyclical chaotic intervals $\{I_1, I_2, I_3, I_4\}$ and as has *G*, $\{J_1, J_2, J_3, J_4\}$ (where $J_i = \varphi(I_i)$ for *i* = 1, 2, 3, 4), so that the map *T* is also chaotic, having 16-cyclical chaotic rectangles belonging to the cartesian product $\{I_1, I_2, I_3, I_4\} \times \{J_1, J_2, J_3, J_4\}$.

References

Arrow, K. J. and Debreu, G., 1954, "Existence of equilibrium for a competitive economy", *Econometrica* 22:265-290

Bischi, G. I., Mammana, C., and Gardini, L., 2000, "Multistability and cyclic attractors in duopoly games", *Chaos, Solitons & Fractals* 11:543-564

Palander, T., 1936, "Instability in competition between two sellers", in Abstracts of Papers Presented at the Research Conference on Economics and Statistics held by the Cowles Commission at Colorado College, *Colorado College Publications*, General Series No. 208, Studies Series No. 21.

Palander, T, 1939, "Konkurrens och marknadsjämvikt vid duopol och oligopol" ("Competition and market equilibrium in duopoly and oligopoly"), *The Scandinavian Journal of Economics* (then Ekonomisk Tidskrift) 41:124-145, and 222-250

Robinson, J., 1933, *The Economics of Imperfect Competition*, MacMillan, London

Sweezy, P. M., 1939, "Demand under conditions of oligopoly", *Journal of Political Economy* 47:568-573

Wald, A., 1936, "Über einige Gleichungssysteme der mathematischen Ökonomie", *Zeitschrift für Nationalökonomie* (Dezember) 637-670